Extremely Slow Spontaneous Electron Trapping in Photodoped *n*-Type CdSe Nanocrystals

Emily Y. Tsui, **Gerard M. Carroll**, **Brigit Miller**, **Arianna Marchioro**, and **Daniel R. Gamelin**
Department of Chemistry, University of Washington, Seattle, WA 98195-1700

Abstract

The trapping dynamics of conduction-band electrons in colloidal degenerately doped *n*-CdSe nanocrystals prepared by photochemical reduction (photodoping) were measured by direct optical methods. The nanocrystals show spontaneous electron trapping with distributed kinetics that extend to remarkably long timescales. Shifts in nanocrystal band-edge potentials caused by quantum confinement and surface ion stoichiometry were also measured by spectroelectrochemical techniques, and their relationship to the slow electron trapping is discussed. The very long electron-trapping timescales observed in these measurements are more consistent with atomic rearrangement than with fundamental electron-transfer processes. Such slow and broadly distributed electron-trapping dynamics are reminiscent of the well-known distributed dynamics of nanocrystal photoluminescence blinking, and potential relationships between the two phenomena are discussed.

Graphical abstract
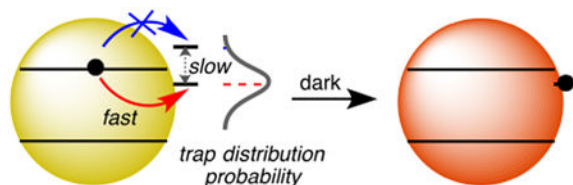
Introduction

Surface traps on colloidal semiconductor nanocrystals (NCs) are exceedingly influential in NC photophysics, luminescence intermittency ("blinking"), photochemistry, and electron transport. Understanding and eventually controlling NC surface traps represents a major unresolved challenge confronting progress toward NC-based electronic and photonic technologies.[1-5] The manifestations of carrier trapping have been studied extensively in the context of photoluminescence (PL) intermittency ("blinking") using single-NC spectroscopies.[6-17] Many models of blinking propose that "off"-state formation occurs *via* carrier trapping at the NC surface, and that this "off" state persists until the surface charge is eliminated.[16-17] Stochastic fluctuations of relative semiconductor band-edge and trap-state

energies have been proposed to explain the distributed "off"-state formation dynamics.[8-10] Similarly, NC delayed luminescence is also hypothesized to involve reversible surface trapping of charge carriers,[18-24] most likely electrons.[20] Several experiments have demonstrated that chemical or electrochemical reduction of NC surface traps can strongly affect PL quantum yields, blinking, and related photodynamics, presumably by turning off otherwise deleterious surface electron-trapping processes.[15, 25-29] Although numerous time-resolved spectroscopic studies have demonstrated sub-nanosecond carrier-trapping rates in CdSe and related semiconductor NCs, both blinking and delayed luminescence measurements routinely show distributed carrier-trapping and detrapping dynamics that extend to seconds or even longer. Rather than reflecting any elementary electron-transfer step, the relatively long blinking "on" times are suggestive of carrier trapping that is gated by another much slower process. To date, there remains little or no direct evidence of such extremely slow charge-carrier trapping in NCs. New approaches to investigating slow charge-carrier trapping in NCs may help to shed light on the processes responsible for these long timescales.

Here, we report extremely slow trapping of conduction-band (CB) electrons (e_{CB}^-) in freestanding colloidal n-type CdSe NCs. e_{CB}^- populations in colloidal n-type CdSe NCs generated via photochemical reduction (photodoping)[30-31] are observed to decay spontaneously on timescales spanning from milliseconds to hours. We show that this slow electron decay is a unimolecular process, ruling out slow NC oxidation by adventitious O_2 or other impurities, and identifying this extraordinarily slow trapping as intrinsic to the NCs themselves. The observation of such extremely slow spontaneous electron trapping in CdSe NCs provides unique opportunities for systematic investigation of the chemical factors affecting this trapping. In preliminary experiments of this type, we show here that this slow electron trapping depends on temperature, consistent with a moderate activation barrier. We also demonstrate that the maximum CdSe NC photodoping level is limited by the photostationary balance between excitation and electron-trapping rates, which in turn depends on NC size and surface stoichiometry. Using $in\ situ$ NC potentiometry,[32] we track the relationship between this slow carrier trapping and NC size, surface stoichiometry, electron occupancy, and Fermi level, providing additional insight into the slow trapping processes. Combined, these results suggest that this very slow electron trapping results from the stochastic appearance of new mid-gap surface traps, similar to previous proposals explaining distributed blinking dynamics. Possible relationships between this slow trapping and the phenomena of PL blinking and delayed luminescence are discussed.

Experimental Section

General Considerations

Unless stated otherwise, all measurements and synthetic manipulations were carried out using standard Schlenk techniques under a nitrogen atmosphere, or in M. Braun or Vac gloveboxes under an atmosphere of purified nitrogen. Anhydrous THF and toluene were purified through columns of activated alumina under argon. All other solvents used were reagent grade or better. Technical grade or reagent grade chemicals were purchased from Sigma-Aldrich or Strem and used without further purification.

Nanocrystal Synthesis

Zinc blende CdSe nanocrystals of various diameters were prepared by an adaptation of a previously reported heat-up synthesis method.[33] As an example: CdO (0.195 g, 1.52 mmol), oleic acid (1.6 mL, 5 mmol), and octadecene (36 g) were combined in a three-necked round bottom flask equipped with a stir bar and condenser and degassed under vacuum at 115 °C for 30 min. Under nitrogen, the mixture was heated to 300 °C until it became optically clear and colorless. The mixture was cooled to 115 °C, and SeO_2 (0.170 g, 1.53 mmol) was added under nitrogen flow, and the mixture was heated to 240 °C for 10 min, becoming an orange solution. The reaction mixture was cooled to room temperature, and the nanocrystals were precipitated using ethanol and then washed via redispersion/precipitation with toluene/ ethanol. For nanocrystals purified under air-free, anhydrous conditions, the crude reaction mixture was distilled to remove octadecene, then dispersed in anhydrous pentane and precipitated with anhydrous methyl acetate.

Surface Treatments of CdSe NCs

The ratios of Cd and Se were changed by an adaptation of the method published by Peng and co-workers.[34] A toluene solution of CdSe NCs prepared as described above was added to a three-necked round-bottom flask equipped with a stir bar and condenser and charged with octadecene (8 mL) and oleylamine (2 mL). The mixture was degassed under vacuum at 100 °C for 30 min, then heated to 140 °C under nitrogen. A dispersion of Se (0.1 mL, ca. 0.1 M in octadecene) was added via syringe, and the mixture stirred at 140 °C for 10 min. This Se treatment was repeated four times, then 0.2 mL of tributylphosphine was added and the mixture was heated to 220 °C for 5 min, then cooled to 35 °C. $Cd(OAc)_2 \cdot 2H_2O$ was added, and the mixture was stirred at 35 °C for 1 h, then precipitated out upon addition of ethanol. The residue was taken up in toluene, stirred with cadmium myristate for 2 h at 60 °C, then dried *in vacuo*. In the glovebox, the residue was dispersed in pentane and filtered to remove excess salts.

General Characterization

Nanocrystals were dried under vacuum, then dispersed in anhydrous toluene and stored in the dinitrogen glovebox. UV-vis spectra were measured using a Varian Cary 5000 spectrophotometer. Low-temperature absorption measurements were carried out using a Cary 5000 spectrophotometer equipped with a fiber-optic cable connected to a dip probe. Energy dispersive X-ray spectrometry (EDS) was measured using a Sirion XL30 scanning electron microscope at the Molecular Analysis Facility of the Molecular Engineering & Sciences Institute at the University of Washington.

Photodoping

CdSe nanocrystals were photodoped as described previously.[30-31] Dispersions of NCs in anhydrous toluene with 30-100 equivalents of $Li[Et_3BH]$ (added as a 0.01 M solution in THF) were prepared anaerobically and loaded into air-free cuvettes equipped with Teflon stir bars. The nanocrystals were photodoped either by illumination with a 100 W Hg/Xe Oriel photolysis lamp (~2 W/cm^2, ~1.5 cm illumination diameter) using a 480 nm long pass filter, or by illumination with a 405 nm diode (50 mW, ~0.06 W/cm^2). In either case, the

solutions were magnetically stirred during excitation. Absorption spectra were monitored during photodoping until the band-edge absorption stopped decreasing. During absorption recovery, the NCs were kept in the dark at room temperature and their absorption spectra were measured at 1 min intervals, unless otherwise stated.

Potentiometry and Spectroelectrochemistry

Fermi levels and nanocrystal redox potentials were measured using the method of spectroelectrochemical potentiometry as detailed previously.[32] Briefly, an air-free septum-capped quartz cuvette was modified by inserting two platinum wires (working and counter electrodes) and a 1 mm Ag/AgCl reference electrode through the septum cap to make a standard three-electrode electrochemical cell. CdSe NCs were suspended in a solution of 0.1 M $[Bu_4N][PF_6]$ in THF, and $Na[Et_3BH]$ was added to the solution in the cuvette in an N_2 glovebox. The samples were then irradiated with supra-band-gap light ($\lambda = 405$ nm, 50 mW). The solution's Fermi level (E_F) was recorded potentiometrically during illumination with a computer-controlled Eco Chemie Autolab II potentiostat. At the same time, the transmittance was measured using a 250 W tungsten halogen lamp directed through an Oriel Cornerstone 74000 monochromator at 590 nm (the peak of the first exciton) and passed through the sample perpendicular to the photodoping excitation source. The transmitted probe light was detected with a Thorlabs PDA 55 Si diode and converted into absorbance through the equation $A = -\log(T/T_0)$, where T is the transmittance through the sample and T_0 is the transmittance absent the sample. T_0 was collected prior to the experiment. A constant baseline measured independently was subtracted from this absorbance, and the resulting absorbance values were then used to calculate $<n>$. The solution was stirred continuously with a magnetic stir bar throughout the measurements. Following the potentiometric measurement, decamethylferrocene was added to the mixture and a cyclic voltammogram was collected as a reference for E_F. All data are plotted against the ferrocenium/ferrocene (Fc^+/Fc) redox couple.

Results and Analysis

(a) Extremely slow intrinsic electron decay

Carboxylate-capped colloidal CdSe NCs were photodoped by excitation with visible light using $Li[Et_3BH]$ as a hole quencher.[30-31] Figure 1A plots the bleach of the first excitonic absorption feature caused by the introduction of delocalized e^-_{CB}. As described previously,[30] this bleach is reversed within seconds upon exposure of the solution to oxidants such as O_2 or decamethylferrocenium ($[FeCp^*_2]^+$). This reversibility is quantitative, with the absorption spectra of the re-oxidized NCs being indistinguishable from those collected before photodoping, ruling out any significant size or compositional changes of the NCs during this process. Figures 1A and 1B show that the CdSe absorption still recovers even in the absence of added oxidant and under rigorously anaerobic conditions, but much more slowly, on the order of minutes or hours. This slow anaerobic e^-_{CB} loss is found to occur with approximately the same rate in the dark as in the light beam of the absorption instrument (see Supporting Information (SI)), indicating that it is not a light-promoted process. It is also observable as a slow brightening of the sample's PL, attributable to diminishing non-radiative Auger

recombination with the loss of e_{CB}^- (see SI), although the PL is undoubtedly also impacted by excess surface-trapped electrons.[30]

A similar slow e_{CB}^- decay has been reported previously for CdSe NCs reduced by addition of ~500-fold excess of the strong reductant sodium biphenyl.[35] In this case, the e_{CB}^- decay was attributed to the presence of trace impurities, exposure to air, or incomplete dryness of the solution,[35] *i.e.*, to extrinsic factors. Extremely slow e_{CB}^- decay was also observed in PbSe NCs reduced by addition of ~100-fold excess cobaltocene.[36] Here, the slow e_{CB}^- decay was attributed to surface electron trapping. In both cases, the kinetics were not analyzable because of the presence of excess chemical reductant in redox equilibrium with the NCs. The present experiments circumvent this limitation, because the reductants used in photodoping are incapable of directly injecting e_{CB}^- into the CdSe NCs.[31] This chemical difference allows e_{CB}^- decay kinetics to be monitored without complication from such additional redox equilibria.

To test the possibility of e_{CB}^- decay due to adventitious O_2, moisture, or other contaminants, solutions of photodoped CdSe NCs were prepared in a nitrogen-filled glovebox (<0.5 ppm O_2, <1.0 ppm H_2O) in dry, deoxygenated solvents. These samples display the same slow e_{CB}^- decay whether stored in Teflon-stoppered cuvettes or in the glovebox. Additionally, mixtures of CdSe NCs and Li[Et$_3$BH] prepared in the dark and stored under nitrogen for 1 day at room temperature still show photodoping to the same extent as freshly prepared samples, ruling out the possibility that small concentrations of adventitious oxidant or slow leaks of air or moisture are responsible for the e_{CB}^- loss observed in Figure 1. Li[Et$_3$BH] decomposes quickly in the presence of moisture and slowly in the presence of dry air (>50% in 24 h).[37] In fact, the NCs can be photodoped again after the anaerobic absorption recovery, indicating that active reducing equivalents are still present after e_{CB}^- loss (Fig. 1C). Corroborating these observations, we find that e_{CB}^- in photodoped ZnO NCs prepared under parallel conditions are stable indefinitely,[38-40] ruling out many possible scenarios involving trace oxidants in the chemicals or glove-box atmosphere. Finally, and most compellingly, the e_{CB}^- decay rate is found to be independent of CdSe NC solution concentration (see SI), which implicates a unimolecular mechanism. These data provide strong evidence that this slow e_{CB}^- decay is *intrinsic* to the NCs themselves.

(b) Nanocrystal size dependence

Figure 2 plots the absorption spectra (solid lines) of a series of zinc blende CdSe NCs of different diameters (d = 2.6–5.6 nm), all prepared using established synthetic procedures[33] and capped by carboxylate ligands. To maintain similar surface compositions, the NC samples were purified *via* the same method of repeated ethanol-precipitation/toluene-resuspension cycles. The dashed lines in Figure 2 correspond to the absorption spectra of these samples collected after photodoping to the maximum possible e_{CB}^- concentration by the incremental addition of Li[Et$_3$BH] and excitation with 405 nm light, *i.e.*, until no further exciton absorption bleach is observed. As we communicated previously,[30] larger CdSe NCs display a greater maximum absorption bleach than smaller ones, reflecting a higher maximum e_{CB}^- population *via* photodoping. Maximum per-NC e_{CB}^- occupancies were

estimated using the relationship $<n> = 2(1 - A/A_0)$, where $<n>$ represents the average number of e^-_{CB} per NC and A and A_0 represent absorbance values at the first excitonic maximum, quantified by multi-peak Gaussian fitting. The resulting values are as follows: for $d = 2.6$ nm, $<n_{max}> = 0.5$; for $d = 3.6$ nm, $<n_{max}> = 1.3$; for $d = 5.6$ nm, $<n_{max}> \sim 2$ (complete bleach of the first excitonic absorption feature). These maximum average electron occupancies correspond to maximum average electron densities of $<N_{max}> = 5.4, 5.3$, and 2.2×10^{19} cm^{-3}, respectively. For comparison, photodoped ZnO NCs display a similar dependence of $<n_{max}>$ on NC diameter, but they can accommodate many more e^-_{CB} per NC ($<N_{max}> \sim 6 \times 10^{20}$ cm^{-3} for all diameters when using Li[Et$_3$BH]).[40]

The data suggest that $<n_{max}>$ in these CdSe NCs is determined by a steady-state balance between photodoping and e^-_{CB} trapping rates under cw photoexcitation, $i.e.$, a photostationary state. We find that the value of $<n_{max}>$ achieved under illumination depends on the specific photoexcitation conditions, and that after photoexcitation is terminated, the e^-_{CB} population decays slowly and asymptotically to a value of $<n>$ that is independent of the excitation rate, $i.e.$, a quasi-equilibrium value ($<n_{equil}>$). Further decay of this quasi-equilibrated e^-_{CB} population is immeasurably slow over several days of observation.

The dependence of $- \; A/A_0$ on photoexcitation rate confirms that $<n_{max}>$ is limited by the rate of e^-_{CB} decay. Figure 3 plots steady-state values of $- \; A/A_0$ for $d \sim 4.0$ nm and $d \sim 2.4$ nm CdSe NCs measured under different 405 nm irradiation powers (proportional to excitation rates). For both NC samples, $- \; A/A_0$ (and hence $<n_{max}>$) is smaller at small excitation rates than at large excitation rates. Moreover, the saturation of $- \; A/A_0$ at large excitation rates implies that the rate of e^-_{CB} decay increases sharply with increasing $<n>$ under those conditions. This increase in e^-_{CB} trapping rates could suggest additional depletion pathways of the conduction-band electrons or of trapped electrons to regenerate empty trap states. Possible pathways might include Shockley-Read-Hall or Auger recombination processes. We note, however, that the observation of $<n_{max}> \sim 0.32$ in the $d = 2.4$ nm CdSe NCs of Figure 3 eliminates the hypothesis[41] that NC photodoping is limited to one electron per NC by rapid Auger recombination because this nonradiative process does not turn on until an e^-_{CB} has been deposited, so photodoping should continue until at least $<n> = 1$ in this scenario. The conditions used for Figure 3 correspond to NC excitation rates up to $\sim$150 excitations•s^{-1} (see SI for calculations), which implies e^-_{CB} trapping on timescales as short as milliseconds at excitation powers where saturation is observed. This trapping rate is far greater than observed in Figure 2, indicating an extremely broad distribution of electron-trapping kinetics.

After maximum photodoping, solutions of n-CdSe NCs of different sizes were stored in the dark under anaerobic conditions, and their absorption spectra were measured periodically over several hours. The inset to Figure 2 shows the dark recovery of the band-edge absorption measured at room temperature over the first 2 h for each sample, plotted as $- \; A/A_0$ vs time. The kinetics of e^-_{CB} loss are similar for all three NCs, but such similar e^-_{CB} decay kinetics are not always observed (see SI), and they appear to depend on NC processing and handling prior to photodoping in a complex way. The decay data for all three NC samples of Figure 2 are fit reasonably well to the same double-exponential function with

time constants of $\tau_1 \sim 7$ min and $\tau_2 \sim 80$ min, and with similar amplitudes (see SI). Their difference comes from their apparent asymptotes, which increase from $<n_{equil}> = 0.05$ to 0.53 to 0.88 across this series (from small to large diameter). This result shows that the highest-energy (most negative potential) CB electrons added to each of these NCs trap at comparable rates, but also that the lowest-energy CB electrons in large CdSe NCs trap far more slowly than the lowest-energy CB electrons in small CdSe NCs do.

(c) Nanocrystal surface chemistry

Monitoring e_{CB}^- decay *via* absorption spectroscopy provides a relatively simple and direct tool for studying the effects of NC surface perturbations on $<n_{max}>$, $<n_{equil}>$, and the e_{CB}^- trapping kinetics of the colloidal ensemble. For example, we find that growth of a ZnS shell over the CdSe NCs significantly increases $<n_{max}>$ and $<n_{equil}>$, and slows e_{CB}^- decay at short times (see SI), consistent with elimination of surface electron traps. This result is similar to the effect of CdSe shell growth over PbSe NCs.[36]

Beyond demonstrating suppressed trapping, we hypothesized that such measurements might provide a unique way to investigate the microscopic nature of native CdSe surface traps. For example, we find that CdSe NCs purified under nitrogen atmosphere display the same recovery characteristics as those purified under ambient conditions, ruling out any influence of surface oxidation on this electron trapping. Importantly, the addition of typical hydrophobic ligands such as trioctylphosphine, octylamine, or trioctylphosphine oxide (technical grade, 90%, containing phosphinic acids) to the NC solutions also does not have any noticeable effect on the trapping kinetics (see SI). These data, along with the NC-concentration independence of the electron-trapping rates, suggest that this e_{CB}^- trapping is not impacted by ligand association/dissociation equilibria.

In contrast, we find that changing the surface Cd^{2+}:Se^{2-} ratio has a large impact. Surface stoichiometry has previously been shown to significantly affect the PL quantum yields of CdSe NCs, primarily attributed to changes in the densities of selenide-derived hole traps.[34, 42-44] Recently, we reported that surface stoichiometry also dramatically affects CdSe NC band-edge potentials, with tunability exceeding ~ 0.4 V,[45] but electron trapping was not examined. Comparably large effects have also been observed elsewhere following various surface modifications.[46-48] Here, in one set of experiments, we treated CdSe NCs with elemental selenium and oleylamine in octadecene to prepare selenium-enriched CdSe NCs (PLQY $\sim 0\%$).[34, 42] We anticipate that surface selenium exists as Se^{2-} during the photodoping experiments, because $Li[Et_3BH]$ can reduce elemental selenium to Li_2Se.[49] This Se^{2-}-enriched sample was then treated with cadmium acetate to passivate the surface Se^{2-} sites and form Cd^{2+}-enriched CdSe NCs (PLQY $\sim 7\%$). Figure 4A plots absorption spectra of the as-prepared CdSe NCs before photodoping, the photodoped Se^{2-}-enriched CdSe NCs from the same batch, and the photodoped Cd^{2+}-enriched NCs prepared as described above. At the same NC concentration, a smaller steady-state absorption bleach is observed for the Se^{2-}-enriched NCs than for the Cd^{2+}-enriched NCs, indicating a smaller $<n_{max}>$, consistent with our previous report.[45] The inset of Figure 4A plots the recovery of excitonic absorption in these Se^{2-}- and Cd^{2+}-enriched NCs over the first hour after photodoping, measured anaerobically at room temperature. These curves again show fairly

similar kinetics but differ in their *y*-asymptotes, which correspond to $<n_{equil}> = 0.08$ and 0.30 for the Se^{2-}- and Cd^{2+}-enriched NCs, respectively. In Figure 4B, the excitonic absorption recovery data from Figure 4A are plotted on log-log axes. As discussed above, the trapping kinetics also extend to faster timescales than those depicted here, reaching at least milliseconds. Clearly, CdSe NCs exhibit extraordinarily broadly distributed e_{CB}^-- trapping dynamics.

(d) Potentiometry

To understand the role of surface-ion enrichment in this electron trapping, we performed spectroelectrochemical potentiometric measurements on the freestanding colloidal CdSe NCs.[32] These measurements allow the changes in NC Fermi level to be quantified during photodoping and subsequent carrier trapping, as a function of the surface modifications described in Figure 4.

Figure 5 compares transient potentiometric data for Se^{2-}- and Cd^{2+}-enriched CdSe NCs collected before, during, and after photodoping in the presence of $Na[Et_3BH]$. Prior to irradiation ($t = 0$ min), the Se^{2-}-enriched NCs already display a resting potential >280 mV more negative than that of the Cd^{2+}-enriched NCs. Upon irradiation ($t = 1$ min), E_F for both samples shifts ~120 mV more negative before reaching a maximum. At this maximum, $<n_{max}> < 0.1$ for the Se^{2-}-enriched NCs and $<n_{max}> \sim 1.5$ for the Cd^{2+}-enriched NCs. When irradiation is terminated ($t = 5$ min), E_F slowly returns more positive for both NC samples until nearly constant potentials are reached at $<n_{equil}>$. Overall, these plots are thus roughly parallel for the two NC samples, but E_F is nearly 300 mV more negative for the Se^{2-}- enriched NCs than for the Cd^{2+}-enriched NCs at all stages of photodoping and recovery. Importantly, these data also demonstrate that electron trapping after termination of the photoexcitation is accompanied by a positive shift of E_F. We further note that the Cd^{2+}- enriched NCs return to approximately their initial E_F after recovery, but the Se^{2-}-enriched NCs plateau at a value of E_F that is >100 mV more positive than it was before photodoping. This observation suggests that the cycle of photodoping followed by electron trapping alters the surfaces of the Se^{2-}-enriched NCs significantly.

(e) Temperature dependence

The temperature dependence of this slow electron trapping was also measured. Reducing the temperature to 20 K has already been reported to stabilize e_{CB}^- dramatically in chemically reduced CdSe NCs,[35] again in the presence of excess reductant. To explore the effect of temperature here, we performed photodoping and recovery measurements at a series of temperatures at which these NC solutions remain in the liquid phase. Toluene solutions of $d \sim 3.6$ nm CdSe NCs were cooled below room temperature (–80 to 20 °C), photodoped to $<n_{max}>$ by exciting with 405 nm light after treatment with $Li[Et_3BH]$, and the recovery of the band-edge absorbance was measured. Figure 6 plots $-A/A_0$ *vs* time for measurements performed at four different temperatures. At $t = 0$ min, a significant increase in the steady-state value of $-A/A_0$ is observed as the temperature is lowered (see SI), indicating a shift in the photostationary state consistent with slower e_{CB}^- trapping at lower temperatures. Slower e_{CB}^- trapping is confirmed directly by the slower recovery in $-A/A_0$ with decreasing temperature after irradiation is terminated. To quantify this temperature dependence, these

decay data were fitted to single-exponential functions to extract approximate e_{CB}^- decay rate constants (see SI), although the true dynamics are obviously more complicated, *e.g.*, Figure 4B. Figure 6 (inset) plots these effective decay rate constants in an Eyring plot. Fitting these data (solid line) yields a low transition-state enthalpy of $H^{\ddagger} \sim 3$ kcal/mol (~130 meV) and a small, negative entropic parameter. These parameters indicate that this e_{CB}^- trapping is an activated process with a barrier of ~5 k_BT at room temperature.

Discussion

(a) Slow surface fluctuations gate electron trapping

Numerous photophysical investigations have found electron transfer from the CB of a semiconductor NC to an available surface trap occurs within pico- to nanoseconds.[50-52] Despite the feasibility of such rapid electron transfer, the electron trapping observed here is remarkably slow, with components extending to minutes and even hours. Clearly, the electron-trapping kinetics monitored here do not reflect the rates of the actual elementary electron-transfer steps themselves. Instead, we propose that they report on the *availability* of suitable electron traps. In this scenario, the data suggest that electron traps can spontaneously appear within the CdSe NC band gap, but this appearance is extremely slow. Prior to trap appearance within the band gap, an e_{CB}^- is stable, but upon appearance of a mid-gap trap, that e_{CB}^- disappears rapidly. Within this interpretation, the data show that the spontaneous formation of mid-gap electron traps is thermally activated. It is noteworthy that in all cases, $<n_{max}>$ is close to only one electron per NC, meaning that the e_{CB}^- decay kinetics observed here reflect the appearance of approximately *just one* new mid-gap electron trap per NC. These deductions are the major qualitative conclusions of the present work.

Given these conclusions, we propose that the extremely slow e_{CB}^- trapping described here is consistent with the hypothesis of dynamic fluctuations in relative surface-trap and CB-edge potentials deduced[8-10] from blinking studies. Because of the small numbers of traps involved in the present observations (one per NC), we consider the relevant trap potentials in terms of probability distributions rather than a static mid-gap density of states. For example, a given trap may dynamically sample many different relative potentials, thereby defining its probability distribution. Figure 7 illustrates one such probability distribution, depicted arbitrarily as a Gaussian function that extends both above and below the NC CB edge. The existence of multiple traps fluctuating simultaneously would scale and broaden this probability distribution curve. The actual distributions are unknown, of course, but nonetheless, within this picture, photodoping raises the Fermi level to above the CB edge, filling any traps that exist below that Fermi level at that time. This photodoping thus generates a standing e_{CB}^- population. After photoexcitation is terminated, e_{CB}^- trapping can only occur when a *new* trap appears with a favorable potential for spontaneous electron transfer, but the formation of a new mid-gap trap is very slow because of a ~5 k_BT activation barrier at room temperature. When no new mid-gap traps appear on the experimental time scale (hours to days), the remaining e_{CB}^- population is taken as $<n_{equil}>$. Although qualitative, this interpretation is consistent with all of the experimental results described above.

(b) Size and surface-stoichiometry dependence

The data presented here indicate that e_{CB}^- trapping can be perturbed by shifts in the CB-edge potential induced by quantum confinement or NC surface chemistry. The effect of quantum confinement on electron trapping is also illustrated schematically in Figure 7. Increasing NC confinement shifts the CB-edge potential more negative but does not affect the localized trap-state potentials. Under illumination, steady state is reached at a given E_F dictated by the balance between excitation and trapping rates, which in turn reflects the trap-potential probability distribution. At this E_F, the smaller NCs have a lower $<n_{max}>$. Turning the excitation source off, CB electrons decay from both NCs at similar rates, but the larger NCs retain a larger $<n_{equil}>$. A similar picture can be used to rationalize the effect of surface Se^{2-} or Cd^{2+} enrichment: Se^{2-} enrichment shifts the NC CB-edge potential more negative by 300 to 400 mV (Figure 5 and ref. [45]), increasing the trap probability density at the band edge. This shift increases electron-trapping rates and thereby decreases $<n_{max}>$ and $<n_{equil}>$.

The extremely long electron-trapping timescales observed here are consistent with rapid electron transfer that is gated by slow atomic rearrangement. Microscopically, these processes may relate to the formation or rearrangement of partially oxidized surface selenium species (formed during photodoping by the photogenerated holes) having redox levels within the gap. If selenium-based, then Cd^{2+} enrichment may decrease the total number of such surface electron traps per NC in addition to shifting band-edge potentials relative to trap potentials, which would further increase both $<n_{max}>$ and $<n_{equil}>$. Other potential surface electron traps could include surface Cd^{2+} ions[53] or anion vacancies.[54] It is interesting to note that the thermodynamic parameters calculated[55] for cation and anion vacancy migration on the surfaces of CdSe NCs are in reasonable agreement with (but somewhat larger than) those estimated from the data in Figure 6, considering that the experimental kinetics are not truly mono-exponential and the calculations were performed using a pre-defined surface ligand coverage and without solvent. The data here do not allow more specific identification of the speciation of the surface electron traps, but they do suggest future opportunities for using slow electron trapping measurements to help identify such traps.

(c) Electron trapping and recycling during photodoping

The excitation power dependence shown in Figure 3 demonstrates that $<n_{max}>$ is limited by the kinetic competition between photodoping and electron trapping. This conclusion would seemingly imply a continuous consumption of the reductant (Li[Et$_3$BH]) at steady state, but $<n_{max}>$ does not decrease after hours of photoexcitation, even though only tens of equivalents of Li[Et$_3$BH] per NC are included during photodoping and the nanocrystals are excited many times per second. Moreover, photodoping is still effective even after most e_{CB}^- from a previous round of photodoping have decayed (Figure 1C). Combined, these observations suggest that the reducing equivalents required for photodoping are not removed from the reaction cycle over time, but can be reintroduced to the CB and then trapped again many times. It is reasonable to conclude that surface-trapped electrons can recombine with subsequent photogenerated valence-band (VB) holes in a mechanism such as illustrated in Figure 8,[56] thereby recycling these electrons.

Figure 8 diagrams the various electron-transfer processes proposed to occur here, including (1) initial hole-quenching by the reducing equivalents from the reductant (shown[31] to proceed *via* a dark surface pre-reduction by [Et$_3$BH]$^-$) after photoexcitation, (2) surface electron trapping, and (3) VB-hole quenching from reduced surface traps after another photoexcitation event. Apparently, therefore, hole transfer to the reduced trap is orders of magnitude faster than electron transfer to the oxidized trap. Such kinetic disparity is a strong indication of significant microscopic structural rearrangement upon trap-state oxidation and reduction, consistent with the thermal activation barrier of ~5 k_BT at room temperature seen from the temperature-dependent electron-trapping kinetics.

(d) Possible relationship to blinking and delayed luminescence

It is interesting to consider the possibility that the distributed electron-trapping dynamics observed here may be related to the well-known distributed kinetics of photoluminescence intermittency (blinking) in single colloidal semiconductor NCs,[6-8, 11, 16-17] and to the distributed kinetics in NC delayed luminescence.[18, 20-24, 57] If related, the electron trapping studied here would be analogous to formation of a luminescence "off" state, and hence its dynamics would be analogous to the "on"-state dynamics of blinking measurements. Distributed "on"-state kinetics extending out to seconds or minutes have been documented in blinking measurements,[6-8, 11, 16-17] and various observations may suggest that both the blinking and the delayed luminescence dynamics in CdSe NCs reflect specifically the dynamics of *electron* trapping and de-trapping. For example, application of a reducing potential to raise the Fermi level close to but below the CB can suppress blinking in CdSe/CdS nanocrystals, interpreted as reducing surface electron traps so that they can no longer accept CB electrons,[15] *i.e.*, blocking pathway 2 in Figure 8. Similarly, introduction of a Cu$^+$ dopant as a designer hole trap within a CdSe NC shifts "on"-state probabilities toward shorter times, interpreted as enhancing the probability of surface electron trapping.[20] Likewise, greater delayed luminescence is observed in samples with longer e_{CB}^- lifetimes in their luminescent core excited states.[20, 24] We note that the chemical instability of delocalized holes in CdSe NCs makes it likely that photogenerated holes are also localized during blinking "off" periods and while in the metastable excited states that feed delayed luminescence, but this hole localization does not preclude the blinking or delayed luminescence *dynamics* from being governed by the electron's trapping/detrapping dynamics.

Other aspects of the two measurements are also similar. For example, the "on"-state blinking dynamics are temperature dependent, as observed here for the slow electron trapping, whereas the "off"-state dynamics are not.[8] Some models of blinking invoke slow fluctuations of trap-state potentials relative to the NC band edge to reproduce their characteristic distributed dynamics,[9-10] and a similar picture may apply here as well. Although inconclusive with respect to mechanistic specifics, the many parallels described above appear to support the hypothesis of a general fundamental analogy between the electron trapping observed here and the phenomena of intermittent and delayed luminescence in colloidal semiconductor NCs. Further experiments are necessary to test this hypothesis and explore such potential links in greater detail. At the very least, these data

Author Manuscript

demonstrate conclusively that spontaneous electron trapping can occur on the same extremely long timescales as blinking and delayed luminescence.

Conclusion

Extraordinarily slow intrinsic e_{CB}^- trapping is observed in photodoped colloidal *n*-type CdSe NCs. This trapping displays broadly distributed kinetics spanning from milliseconds to hours. Trapping measurements have been performed under various experimental conditions, with different NC sizes, and with different NC surface stoichiometries, and the results point to an interpretation in which these slow electron-trapping dynamics reflect the thermally activated stochastic appearance of individual mid-gap electron traps, much like has been proposed to explain the distributed dynamics of photoluminescence blinking. Microscopically, the results support a description of this slow electron trapping in which intrinsically fast elementary electron-transfer steps are gated by much slower atomic rearrangements at the NC surfaces.

Supplementary Material

Refer to Web version on PubMed Central for supplementary material.

Acknowledgments

References

1. Hines MA, Guyot-Sionnest P. Synthesis and Characterization of Strongly Luminescing ZnS-Capped CdSe Nanocrystals. J Phys Chem. 1996; 100:468–471.

2. Chen Y, Vela J, Htoon H, Casson JL, Werder DJ, Bussian DA, Klimov VI, Hollingsworth JA. "Giant" Multishell CdSe Nanocrystal Quantum Dots with Suppressed Blinking. J Am Chem Soc. 2008; 130:5026–5027. [PubMed: 18355011]

3. Mahler B, Spinicelli P, Buil S, Quelin X, Hermier JP, Dubertret B. Towards non-blinking colloidal quantum dots. Nat Mater. 2008; 7:659–664. [PubMed: 18568030]

4. van Embden J, Jasieniak J, Gómez DE, Mulvaney P, Giersig M. Review of the Synthetic Chemistry Involved in the Production of Core/Shell Semiconductor Nanocrystals. Aust J Chem. 2007; 60:457–471.

5. Reiss P, Protière M, Li L. Core/Shell Semiconductor Nanocrystals. Small. 2009; 5:154–168. [PubMed: 19153991]

6. Nirmal M, Dabbousi BO, Bawendi MG, Macklin JJ, Trautman JK, Harris TD, Brus LE. Fluorescence intermittency in single cadmium selenide nanocrystals. Nature. 1996; 383:802–804.

7. Kuno M, Fromm DP, Hamann HF, Gallagher A, Nesbitt DJ. Nonexponential "blinking" kinetics of single CdSe quantum dots: A universal power law behavior. J Chem Phys. 2000; 112:3117–3120.

8. Shimizu KT, Neuhauser RG, Leatherdale CA, Empedocles SA, Woo WK, Bawendi MG. Blinking statistics in single semiconductor nanocrystal quantum dots. Phys Rev B. 2001; 63:205316.

9. Tang J, Marcus RA. Mechanisms of fluorescence blinking in semiconductor nanocrystal quantum dots. J Chem Phys. 2005; 123:054704. [PubMed: 16108682]

10. Pelton M, Smith G, Scherer NF, Marcus RA. Evidence for a diffusion-controlled mechanism for fluorescence blinking of colloidal quantum dots. Proc Natl Acad Sci USA. 2007; 104:14249–14254. [PubMed: 17720807]

11. Frantsuzov P, Kuno M, Jánko B, Marcus RA. Universal emission intermittency in quantum dots, nanorods, and nanowires. Nat Phys. 2008; 4:519–522.

12. Zhao J, Nair G, Fisher BR, Bawendi MG. Challenge to the Charging Model of Semiconductor-Nanocrystal Fluorescence Intermittency from Off-State Quantum Yields and Multiexciton Blinking. Phys Rev Lett. 2010; 104:157403. [PubMed: 20482016]

13. Rosen S, Schwartz O, Oron D. Transient Fluorescence of the Off State in Blinking CdSe/CdS/ZnS Semiconductor Nanocrystals Is Not Governed by Auger Recombination. Phys Rev Lett. 2010; 104:157404. [PubMed: 20482017]

14. Califano M. Off-State Quantum Yields in the Presence of Surface Trap States in CdSe Nanocrystals: The Inadequacy of the Charging Model To Explain Blinking. J Phys Chem C. 2011; 115:18051–18054.

15. Galland C, Ghosh Y, Steinbrück A, Sykora M, Hollingsworth JA, Klimov VI, Htoon H. Two types of luminescence blinking revealed by spectroelectrochemistry of single quantum dots. Nature. 2011; 479:203–207. [PubMed: 22071764]

16. Cordones AA, Leone SR. Mechanisms for charge trapping in single semiconductor nanocrystals probed by fluorescence blinking. Chem Soc Rev. 2013; 42:3209–3221. [PubMed: 23306775]

17. Efros AL, Nesbitt DJ. Origin and control of blinking in quantum dots. Nat Nanotech. 2016; 11:661–671.

18. Sher PH, Smith JM, Dalgarno PA, Warburton RJ, Chen X, Dobson PJ, Daniels SM, Pickett NL, O'Brien P. Power law carrier dynamics in semiconductor nanocrystals at nanosecond timescales. Appl Phys Lett. 2008; 92:101111.

19. Jones M, Lo SS, Scholes GD. Quantitative modeling of the role of surface traps in CdSe/CdS/ZnS nanocrystal photoluminescence decay dynamics. Proc Natl Acad Sci USA. 2009; 106:3011–3016. [PubMed: 19218443]

20. Whitham PJ, Knowles KE, Reid PJ, Gamelin DR. Photoluminescence Blinking and Reversible Electron Trapping in Copper-Doped CdSe Nanocrystals. Nano Lett. 2015; 15:4045–4051. [PubMed: 26007328]

21. Rabouw FT, Kamp M, van Dijk-Moes RJA, Gamelin DR, Koenderink AF, Meijerink A, Vanmaekelbergh D. Delayed Exciton Emission and Its Relation to Blinking in CdSe Quantum Dots. Nano Lett. 2015; 15:7718–7725. [PubMed: 26496661]

22. Rabouw FT, van der Bok JC, Spinicelli P, Mahler B, Nasilowski M, Pedetti S, Dubertret B, Vanmaekelbergh D. Temporary Charge Carrier Separation Dominates the Photoluminescence Decay Dynamics of Colloidal CdSe Nanoplatelets. Nano Lett. 2016; 16:2047–2053. [PubMed: 26863992]

23. Whitham PJ, Marchioro A, Knowles KE, Kilburn TB, Reid PJ, Gamelin DR. Single-Particle Photoluminescence Spectra, Blinking, and Delayed Luminescence of Colloidal CuInS2 Nanocrystals. J Phys Chem C. 2016; 120:17136–17142.

24. Marchioro A, Whitham PJ, Knowles KE, Kilburn TB, Reid PJ, Gamelin DR. Tunneling in the Delayed Luminescence of Colloidal Semiconductor Nanocrystals, and Relationship to Blinking. J Phys Chem C. 2016; 120:27040–27049.

25. Jha PP, Guyot-Sionnest P. Electrochemical Switching of the Photoluminescence of Single Quantum Dots. J Phys Chem C. 2010; 114:21138–21141.

26. Qin W, Shah RA, Guyot-Sionnest P. CdSeS/ZnS Alloyed Nanocrystal Lifetime and Blinking Studies under Electrochemical Control. ACS Nano. 2012; 6:912–918. [PubMed: 22191620]

27. Weaver AL, Gamelin DR. Photoluminescence Brightening via Electrochemical Trap Passivation in ZnSe and Mn2+-Doped ZnSe Quantum Dots. J Am Chem Soc. 2012; 134:6819–6825. [PubMed: 22417458]

28. Rinehart JD, Weaver AL, Gamelin DR. Redox Brightening of Colloidal Semiconductor Nanocrystals using Molecular Reductants. J Am Chem Soc. 2012; 134:16175–16177. [PubMed: 22985258]

29. Boehme SC, Azpiroz JM, Aulin YV, Grozema FC, Vanmaekelbergh D, Siebbeles LDA, Infante I, Houtepen AJ. Density of Trap States and Auger-mediated Electron Trapping in CdTe Quantum-Dot Solids. Nano Lett. 2015; 15:3056–3066. [PubMed: 25853555]

30. Rinehart JD, Schimpf AM, Weaver AL, Cohn AW, Gamelin DR. Photochemical Electronic Doping of Colloidal CdSe Nanocrystals. J Am Chem Soc. 2013; 135:18782–18785. [PubMed: 24289732]

31. Tsui EY, Hartstein KH, Gamelin DR. Selenium Redox Reactivity on Colloidal CdSe Quantum Dot Surfaces. J Am Chem Soc. 2016; 135:11105–11108.

32. Carroll GM, Brozek CK, Hartstein KH, Tsui EY, Gamelin DR. Potentiometric Measurements of Semiconductor Nanocrystal Redox Potentials. J Am Chem Soc. 2016; 138:4310–4313. [PubMed: 26978480]

33. Chen O, Chen X, Yang Y, Lynch J, Wu H, Zhuang J, Cao YC. Synthesis of Metal–Selenide Nanocrystals Using Selenium Dioxide as the Selenium Precursor. Angew Chem Int Ed. 2008; 47:8638–8641.

34. Gao Y, Peng X. Photogenerated Excitons in Plain Core CdSe Nanocrystals with Unity Radiative Decay in Single Channel: The Effects of Surface and Ligands. J Am Chem Soc. 2015; 137:4230–4235. [PubMed: 25785631]

35. Shim M, Guyot-Sionnest P. N-type colloidal semiconductor nanocrystals. Nature. 2000; 407:981–983. [PubMed: 11069172]

36. Koh WK, Koposov AY, Stewart JT, Pal BN, Robel I, Pietryga JM, Klimov VI. Heavily doped n-type PbSe and PbS nanocrystals using ground-state charge transfer from cobaltocene. Sci Rep. 2013; 3:2004. [PubMed: 23774224]

37. Brown HC, Krishnamurthy S, Hubbard JL. Addition compounds of alkali metal hydrides. 15. Steric effects in the reaction of representative trialkylboranes with lithium and sodium hydrides to form the corresponding trialkylborohydrides. J Am Chem Soc. 1978; 100:3343–3349.

38. Liu WK, Whitaker KM, Kittilstved KR, Gamelin DR. Stable Photogenerated Carriers in Magnetic Semiconductor Nanocrystals. J Am Chem Soc. 2006; 128:3910–3911. [PubMed: 16551089]

39. Liu WK, Whitaker KM, Smith AL, Kittilstved KR, Robinson BH, Gamelin DR. Room-Temperature Electron Spin Dynamics in Free-Standing ZnO Quantum Dots. Phys Rev Lett. 2007; 98:186804. [PubMed: 17501594]

40. Schimpf AM, Gunthardt CE, Rinehart JD, Mayer JM, Gamelin DR. Controlling Carrier Densities in Photochemically Reduced Colloidal ZnO Nanocrystals: Size Dependence and Role of the Hole Quencher. J Am Chem Soc. 2013; 135:16569–16577. [PubMed: 24050304]

41. Shim M, Guyot-Sionnest P. Organic-Capped ZnO Nanocrystals: Synthesis and n-Type Character. J Am Chem Soc. 2001; 123:11651–11654. [PubMed: 11716721]

42. Jasieniak J, Mulvaney P. From Cd-Rich to Se-Rich - the Manipulation of CdSe Nanocrystal Surface Stoichiometry. J Am Chem Soc. 2007; 129:2841–2848. [PubMed: 17309253]

43. Anderson NC, Hendricks MP, Choi JJ, Owen JS. Ligand Exchange and the Stoichiometry of Metal Chalcogenide Nanocrystals: Spectroscopic Observation of Facile Metal-Carboxylate Displacement and Binding. J Am Chem Soc. 2013; 135:18536–18548. [PubMed: 24199846]

44. Busby E, Anderson NC, Owen JS, Sfeir MY. Effect of Surface Stoichiometry on Blinking and Hole Trapping Dynamics in CdSe Nanocrystals. J Phys Chem C. 2015; 119:27797–27803.

45. Carroll GM, Tsui EY, Brozek CK, Gamelin DR. Spectroelectrochemical Measurement of Surface Electrostatic Contributions to Colloidal CdSe Nanocrystal Redox Potentials. Chem Mater. 2016; 28:7912–7918.

46. Brown PR, Kim D, Lunt RR, Zhao N, Bawendi MG, Grossman JC, Bulovic V. Energy Level Modification in Lead Sulfide Quantum Dot Thin Films through Ligand Exchange. ACS Nano. 2014; 8:5863–5872. [PubMed: 24824726]

47. Jeong KS, Deng Z, Keuleyan S, Liu H, Guyot-Sionnest P. Air-Stable n-Doped Colloidal HgS Quantum Dots. J Phys Chem Lett. 2014; 5:1139–1143. [PubMed: 26274461]

48. Schimpf AM, Knowles KE, Carroll GM, Gamelin DR. Electronic Doping and Redox Potential Tuning in Colloidal Semiconductor Nanocrystals. Acc Chem Res. 2015; 48:1929–1937. [PubMed: 26121552]

49. Gladysz JA, Hornby JL, Garbe JE. Convenient one-flask synthesis of dialkyl selenides and diselenides via lithium triethylborohydride reduction of Se_x. J Org Chem. 1978; 43:1204–1208.

50. Knowles KE, McArthur EA, Weiss EA. A Multi-Timescale Map of Radiative and Nonradiative Decay Pathways for Excitons in CdSe Quantum Dots. ACS Nano. 2011; 5:2026–2035. [PubMed: 21361353]

51. Kern SJ, Sahu K, Berg MA. Heterogeneity of the Electron-Trapping Kinetics in CdSe Nanoparticles. Nano Lett. 2011; 11:3493–3498. [PubMed: 21780773]

52. Morris-Cohen AJ, Frederick MT, Cass LC, Weiss EA. Simultaneous Determination of the Adsorption Constant and the Photoinduced Electron Transfer Rate for a Cds Quantum Dot–Viologen Complex. J Am Chem Soc. 2011; 133:10146–10154. [PubMed: 21618976]

53. Zhao J, Holmes MA, Osterloh FE. Quantum Confinement Controls Photocatalysis: A Free Energy Analysis for Photocatalytic Proton Reduction at CdSe Nanocrystals. ACS Nano. 2013; 7:4316–4325. [PubMed: 23590186]

54. Chestnoy N, Harris TD, Hull R, Brus LE. Luminescence and photophysics of cadmium sulfide semiconductor clusters: the nature of the emitting electronic state. J Phys Chem. 1986; 90:3393–3399.

55. Voznyy O, Sargent EH. Atomistic Model of Fluorescence Intermittency of Colloidal Quantum Dots. Phys Rev Lett. 2014; 112:157401. [PubMed: 24785069]

56. Shockley W, Read WT. Statistics of the Recombinations of Holes and Electrons. Phys Rev. 1952; 87:835–842.

57. Tachiya M, Seki K. Unified explanation of the fluorescence decay and blinking characteristics of semiconductor nanocrystals. Appl Phys Lett. 2009; 94:081104.
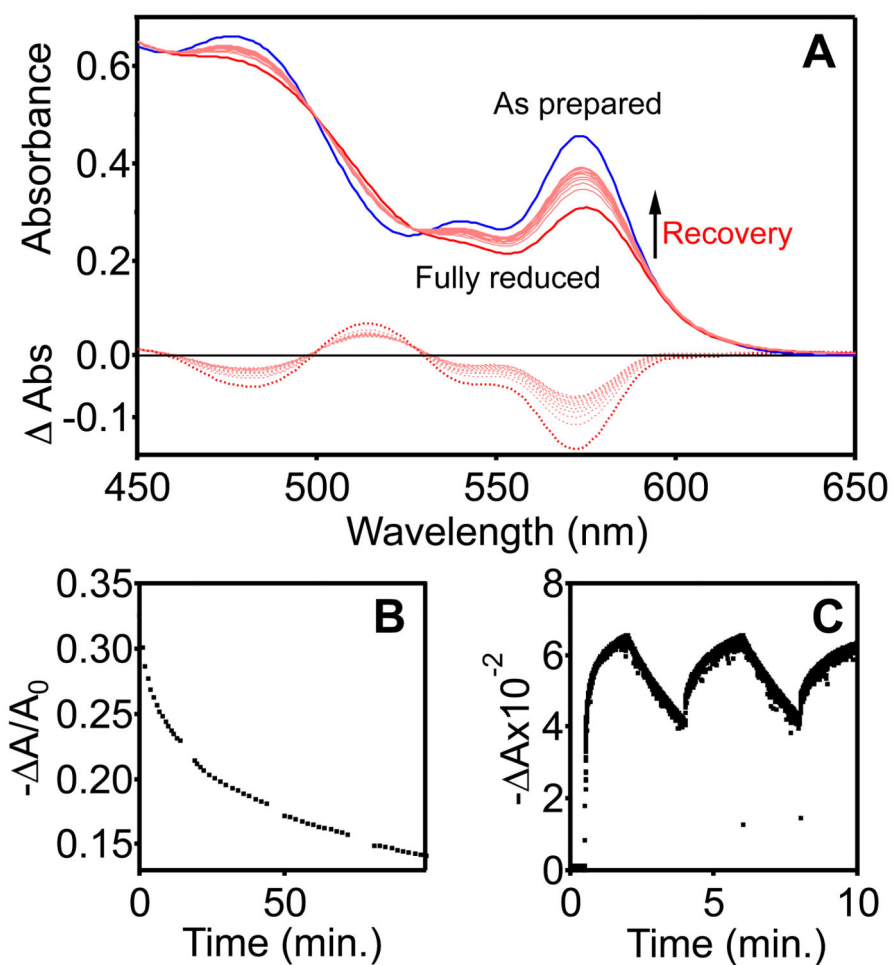
Figure 1.
(A) Absorption spectra of photodoped CdSe NCs at room temperature measured over 90 min (NC diameter = ~3.6 nm, concentration = 2.8 μM in toluene). (B) Normalized first-exciton differential absorbance ($-\Delta A/A_0$, $\lambda = 573$ nm) plotted *vs* time, where A_0 represents the exciton absorbance prior to photodoping. (C) First-exciton differential absorbance ($-\Delta A$, $\lambda = 580$ nm) of CdSe NCs ($d \sim 3.8$ nm) in toluene with added Li[Et$_3$BH]. The sample was excited using a 405 nm LED (50 mW) which was switched on and off at 2 min intervals.
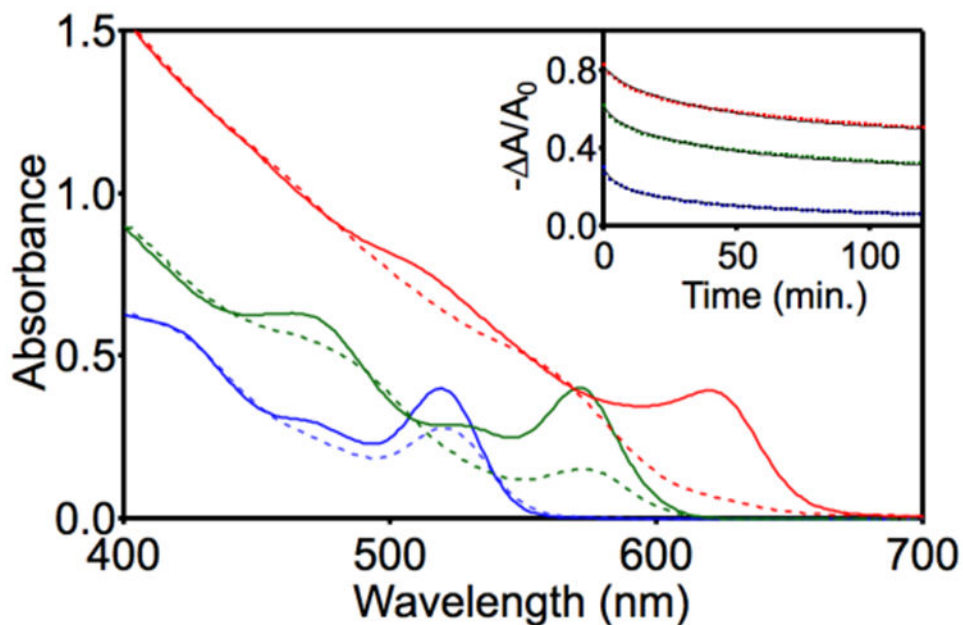
Figure 2.
Absorption spectra of CdSe NCs of various diameters, measured before (solid lines) and after photodoping (dashed lines) using Li[Et$_3$BH] as the reductant and 405 nm irradiation for excitation. d = 5.6 nm (red), 3.6 nm (green), and 2.6 nm (blue). Inset: Normalized first-exciton differential absorbance ($-\Delta A/A_0$) of these photodoped CdSe nanocrystals plotted *vs* time over the first 2 h after 405 nm irradiation is terminated (at t = 0). The black curves in the inset depict double-exponential fits to the data using $\tau_1 \sim 7$ min and $\tau_2 \sim 80$ min, and different asymptotes (see text).
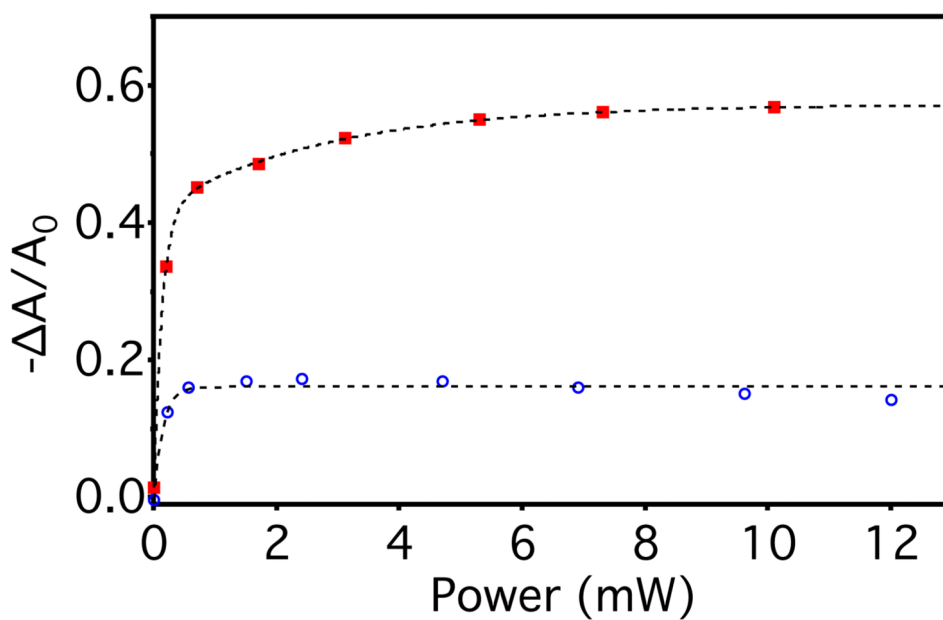
Figure 3.
Normalized differential first-exciton absorbance ($-\Delta A/A_0$, λ = 586 or 518 nm) of CdSe NCs of two sizes ($d \sim 4.0$ nm, red squares, or $d \sim 2.4$ nm, blue circles) in toluene with added Li[Et$_3$BH] (60 equiv/NC or 7 equiv/NC, respectively) under 405 nm illumination at various CW excitation powers. The dashed lines are guides to the eye.
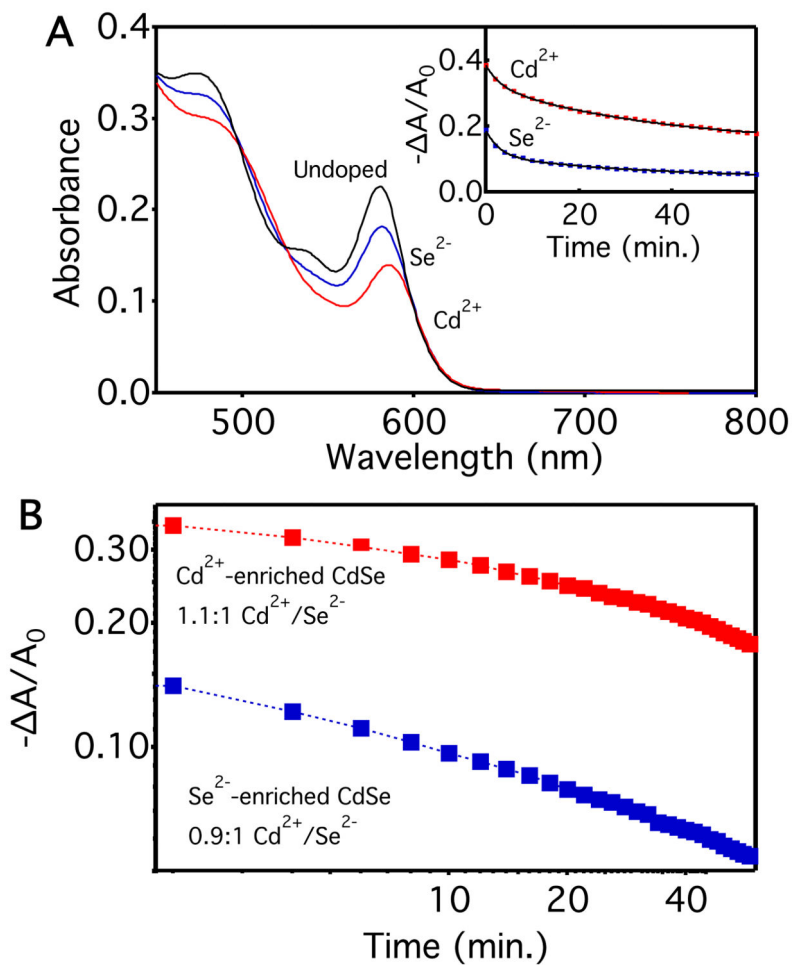
Figure 4.
(A) Absorption spectra of photodoped CdSe NCs (cores $d \sim 3.9$ nm) after Se^{2-} and Cd^{2+} enrichment. Inset: Normalized first-exciton differential absorbance ($- \Delta A/A_0$, $\lambda = 581$, and 585 nm for Se^{2-}-enriched, and Cd^{2+}-enriched NC samples respectively) measured over 60 min at room temperature for CdSe NCs with the different surface compositions. The black lines depict double exponential fits as described in the text ($\tau_1 \sim 3$ min, $\tau_2 \sim 35$ min). (B) The excitonic absorption recovery data from the inset of panel (A), plotted vs time in a log-log representation. Cd^{2+}/Se^{2-} ratios measured using energy-dispersive X-ray spectroscopy (EDS) are listed for each sample.
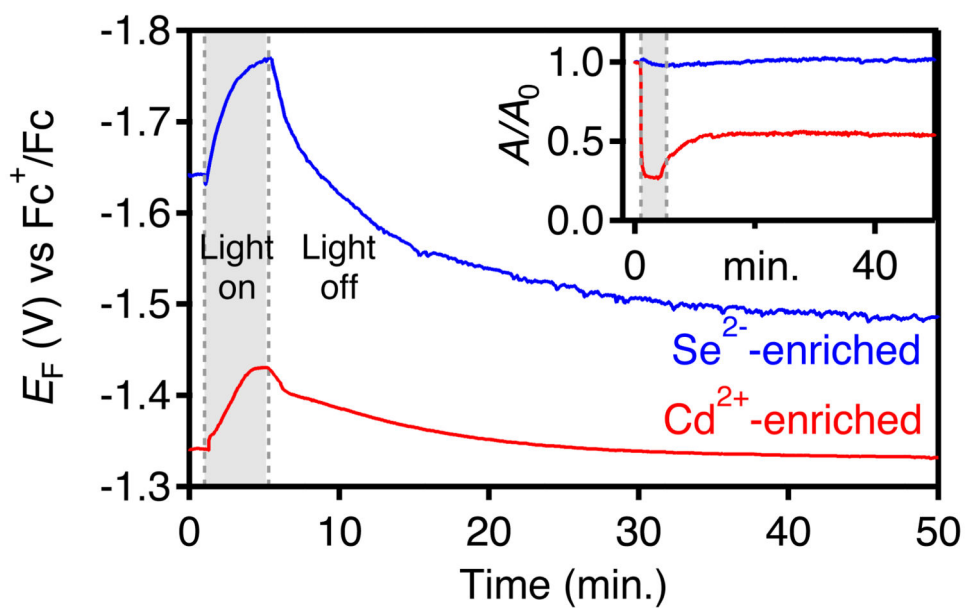
Figure 5.
Transient potentiometric data for photodoping $d = 3.8$ nm Cd^{2+}-enriched (red) and Se^{2-}-enriched (blue) CdSe NCs with $Na[Et_3BH]$ as the hole quencher in a THF solution with 0.1 M $TBAPF_6$ as the supporting electrolyte. For each sample, the NCs were photodoped using a 405 nm diode (50 mW) between $t = 1$ and 5 min. At $t = 5$ min, photoexcitation was stopped but E_F was monitored further. Inset: A/A_0 collected in concert with E_F.
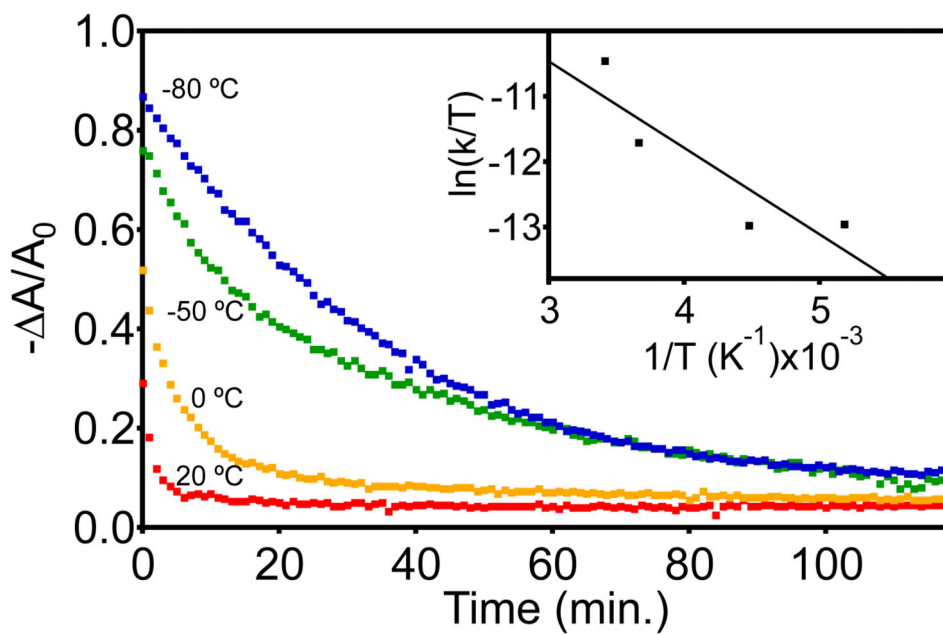
Figure 6.

Normalized excitonic bleach ($-\Delta A/A_0$) recovery data for photodoped d = ~3.6 nm CdSe NCs measured at 20, 0, −50, and −80 °C. Inset: Eyring plot of the rate constants estimated from single-exponential fits of the absorption recovery data. R^2 = 0.81. Fitting yields $\Delta H^{\ddagger}$ ~ 3 kcal/mol and a small, negative entropic parameter. These parameters correspond to an activation barrier of ~5 k_BT at room temperature.
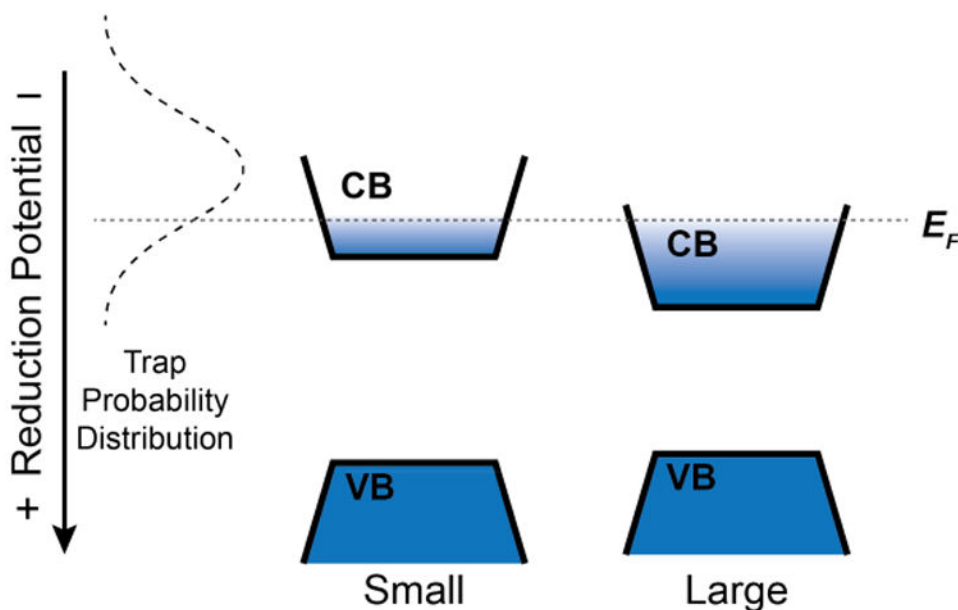
Figure 7.
Schematic depiction of the proposed relationship between a trap potential's probability distribution and the photodoping characteristics of colloidal CdSe NCs. The dashed Gaussian curve depicts the probability distribution of a single trap's potential, which fluctuates stochastically relative to the CB edge. Within this distribution, a trap has a discrete relative potential for a period of time before hopping to another relative potential. Sampling of the full potential distribution is slow and thermally activated. The dotted horizontal line indicates the Fermi level achieved *via* photodoping. When the trap hops to a potential below the Fermi level, electron transfer from the CB to the trap is favorable. Under steady-state excitation conditions, the photodoping rate equals the electron-trapping rate. Increasing quantum confinement shifts the CB edge to more negative potentials, increasing the probability of thermodynamically favorable electron trapping at a given value of $<n>$, yielding a smaller value of $<n_{max}>$. *A* similar schematic applies to nanocrystal redox-potential shifting *via* surface non-stoichiometries. Surface perturbations likely also affect the total number of fluctuating trap states per NC, which in turn affects photodoping and electron decay, but these considerations are not depicted here.
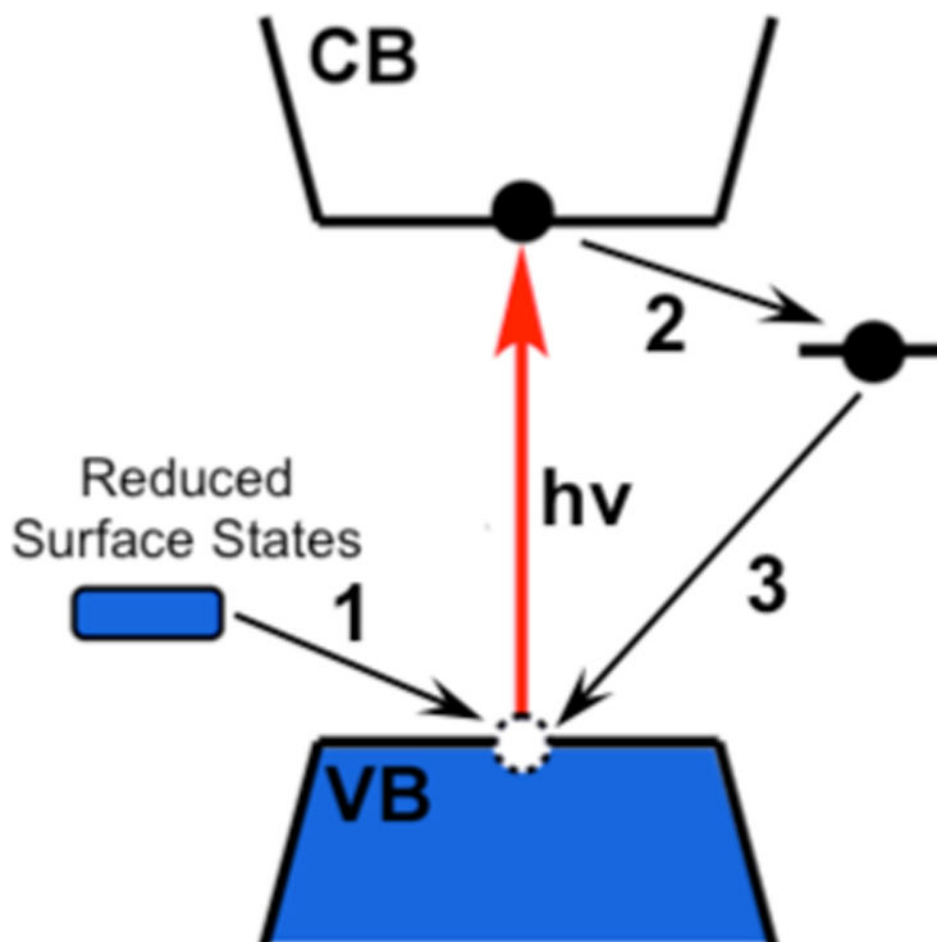
Figure 8.
Diagram of electron-transfer processes observed during CdSe NC photodoping and subsequent electron trapping. (1) Under irradiation, the valence-band holes of CdSe NCs are initially quenched *via* electron transfer from reduced surface states derived from the triethylborohydride reductant (ref. [31]). (2) Conduction-band electrons transfer to mid-gap surface traps. (3) Electrons transfer from reduced surface traps to the valence band to quench subsequent photogenerated holes.